How to cite: *Angew. Chem. Int. Ed.* **2021**, *60*, 18838–18844
International Edition: doi.org/10.1002/anie.202107034
German Edition: doi.org/10.1002/ange.202107034

Cyclic Peptides

Molecular Plumbing to Bend Self-Assembling Peptide Nanotubes

*Federica Novelli, Marcos Vilela, Antía Pazó, Manuel Amorín, and Juan R. Granja**

Abstract: *Light-induced molecular piping of cyclic peptide nanotubes to form bent tubular structures is described. The process is based on the [4+4] photocycloaddition of anthracene moieties, whose structural changes derived from the interdigitated flat disposition of precursors to the corresponding cycloadduct moieties, induced the geometrical modifications in nanotubes packing that provokes their curvature. For this purpose, we designed a new class of cyclic peptide nanotubes formed by β- and α-amino acids. The presence of the former predisposes the peptide to stack in a parallel fashion with the β-residues aligned along the nanotube and the homogeneous distribution of anthracene pendants.*

Introduction

Light is the livelihood that provides not only thermal heating support but also triggers a variety of essential transformations for living organisms.[1] An array of chemical processes, i.e., bioenergy production through photosynthesis, the breakage or formation of chemical bonds, or changes in conformation, are pivotal photoinduced events for living organisms.[2] The visual transduction pathway based on rhodopsin photoisomerization is one of the remarkable examples at this respect. Rhodopsin is the binary complex involved in visual transduction through the isomerization of retinal, from 11-*cis*- to all-*trans*-isomer, upon light irradiation (Scheme 1 a).[3] Such isomerization gives rise to opsin conformational changes that induce the neuronal excitation involved in the visual pathway. In recent years, supramolecular processes have dealt with dynamic systems that complement the originally more static complexes based on the more stable thermodynamic structure. Therefore, system chemistry, far from equilibria processes, kinetic traps, dissipative assembly or dynamic libraries, have emerged as new tools for developing functional supramolecular systems.[4] In this sense, responsive materials are a paradigm in materials sciences due

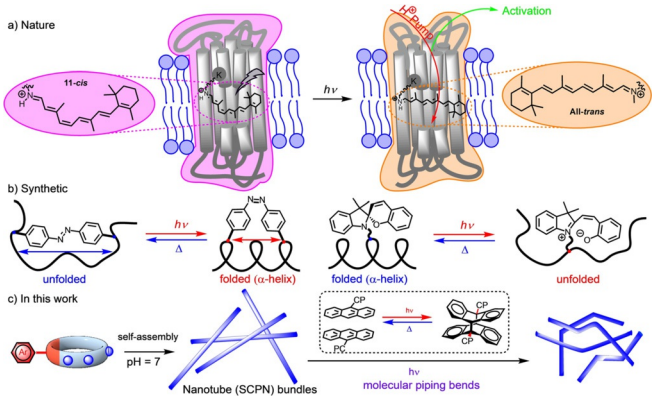

Scheme 1. Light-induced geometrical changes of a) Rhodopsin, b) azo,[15] and spiropyran[16] compounds as initiators of molecular changes, and c) the nanotube plumbing technology developed in this work based on anthracene [4+4] photodimerization.

to the ability to modify their properties in response to external inputs.[5] Thus, materials sensitive to pH, redox, ionic strength, or temperature changes have been pursued in the last years, seeking a variety of functions and applications. In this respect, light-responsive materials represent a class of versatile materials in which the use of appropriate wavelength can induce on-demand changes in their shape, size, or conformation.[4a,6] In general, isomerizations (*E*/*Z*), electrocyclizations, or cycloaddition processes provide the required molecular modifications to change the material properties (Scheme 1 b).[7]

Tube-shaped materials are very useful components, both at the macroscopic and microscopic levels, as structural components or for conveying flowing substances thanks to the hollow structure and lightness. In most cases, to improve the tube functions, plumbing actions to pipe elbows or bends are required. At the molecular level, it is still required to create this kind of adapters or engineering on-demand "molecular plumbing processes" to adapt the nanotube shape to the surrounding media to improve its applications.[8,9]

Self-assembling cyclic peptide nanotubes (SCPNs) are a class of supramolecular polymers made by the ordered piling up of peptide macrocycles.[10] A large variety of applications have been developed since its discovery in 1993.[11] Especially relevant are those related to ion and molecular transport in which the properties of the nanotube pore provide some selectivity.[12] Kinetic studies suggest that nanotube formation is a cooperative process in which once nanotube formation is triggered, they continue growing, helped by the inter-tube (crystal lattice) interactions, making difficult to control nanotube length and packing.[13] Although some steps towards this end have been achieved in the last

[*] Dr. F. Novelli, M. Vilela, A. Pazó, Dr. M. Amorín, Prof. Dr. J. R. Granja
Centro Singular de Investigación en Química Biolóxica e Materiais Moleculares (CIQUS) and Organic Chemistry Department
Universidade de Santiago de Compostela
15782 Santiago de Compostela (Spain)
E-mail: juanr.granja@usc.es
Supporting information and the ORCID identification number(s) for the author(s) of this article can be found under: https://doi.org/10.1002/anie.202107034.

years by using CPs/polymers hybrids,[14] further control in these nanotube structural parameters are still required.

Recent studies by us and others have opened the opportunity to create stimuli reversible SCPN structures that might help to develop artificial cell cytoskeletons and other dynamic scaffolds.[17] For these purposes, we have combined the interpeptide interactions based on amide hydrogen-bonded networks and the π–π interactions of pyrene (Pyr) moieties to trigger nanotube formation in aqueous or droplet media.[18,17b] In these peptides, the interdigitation of the aromatic moieties helps not only in the CP stacking to form nanotubes but also promotes the formation of small bundles through a hierarchical self-assembling process (Scheme 2). In

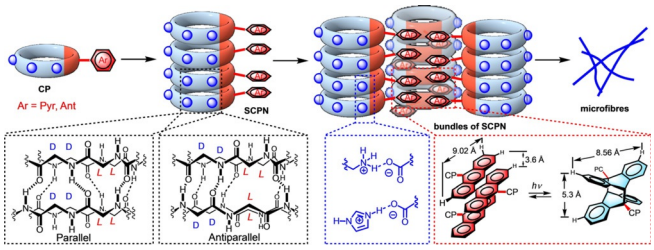

Scheme 2. Supramolecular hierarchical process responsible for SCPN formation. Right inset, proposed changes in dimensions of anthracene moieties upon photodimerization.

this strategy, the aryl group can be orthogonally introduced at the end of the process by condensing aryl aldehydes with CPs bearing an alkoxyamine moiety.[18,17b] Although the incorporation of the aromatic ring facilitates the stacking of CP rings, the distance differences between the π-stacking (3.3–3.5 Å) and β-sheet peptide strands (4.7 Å) also facilitate the intertube packing by interdigitating their aromatic moieties. In this regard, we have shown that trimeric silver clusters help to stabilize the tubular structure through the intercalation on the pyrene packing.[19] Therefore, aryl pendants represent an additional checkpoint to tune nanotube formation and properties. We envisaged that anthracene (Ant) moiety could also be used, dampening the hydrophobic effect in the assembly process while maintaining good luminescent behavior and stability.[20] Besides, this group is a photoactive material that can dimerize using appropriate wavelength,[21] being used in various supramolecular contexts, especially for cross-linking purposes.[22] We envisioned that the change in volume and dimensions between the stacked dimer of Ant and the corresponding photodimer could be used to induce changes in the SCPN packing and properties (Scheme 2).[23] Such nanotube movement could be implemented in developing photosensitive materials.[24] Therefore, we speculated that the use of this reversible process could provide a new tool to modify nanotube shapes and functions. Herein, we provide the first step for the on-demand molecular plumbing of peptide nanotubes.

Results and Discussion

To carry out this work, we decided to create a new class of peptide hybrids made of α- and β-amino acids to precisely control not only the interpeptide register but also to control the β-sheet type (Scheme 3).[25,26] For this purpose, we used

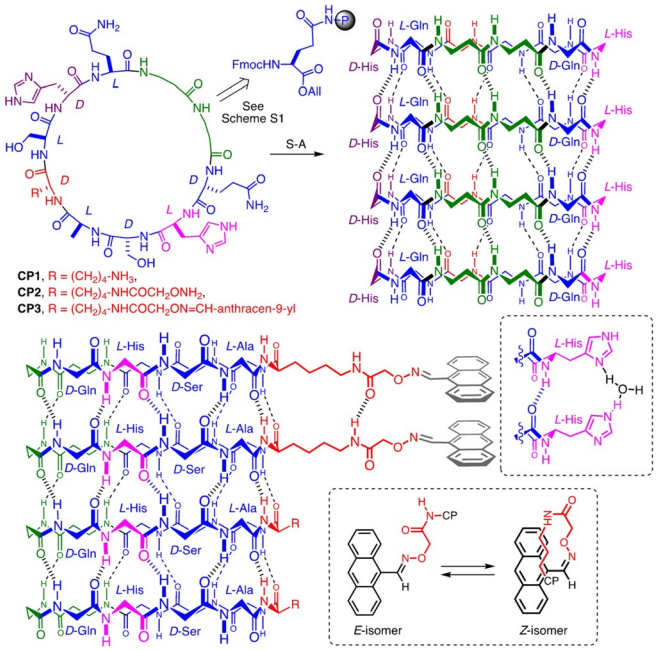

Scheme 3. Structure of cyclic peptides and models for nanotube formation guided by the stacking of anthracene moiety and β-residues (in green). Bottom inset: proposed *E*/*Z* isomer of oxime linker to explain the observed Ant ring current shielding of Lys side-chain signals. Top inset: proposed His-His interaction mediated by a water molecule.

the original D,L-alternating sequence[11] combined with two β-amino acids. In the required flat conformation, this type of residues with an even number of carbons between the carbonyl and NH moieties predispose the amide groups (NH and C=O) to point out in the opposite way.[27] Therefore, the insertion of these β-residues should induce the CPs to stack, forming parallel β-sheet structures.[28] The incorporation of the His residues was aimed to provide solubility to the peptide and self-assembling fulminant capability due to its ionization state changes at almost neutral pH. Besides, a Lys modified with a hydroxylamine acetyl moiety was place at the opposite side of the β-residues to allow the incorporation of the anthracene-9-carbaldehyde through an oxime bond. Consequently, in the proposed parallel model, the arene stacking and the β-residues would provide nanotubes in which each residue would be aligned with itself along the tubular structure (see nanotubes models in Scheme 3). In this organization, His (as illustrated in the inset), Ser or Gln side chains could also participate in stabilizing the tubular structure by forming additional hydrogen bonds assisted, in some cases, by water molecules.

CP2 was prepared by solid-phase methods following the strategy previously reported by our group (Supporting

Information, Scheme S1).[17b,18,29] The resulting pure peptide was condensed with the anthraldehyde by mixing both components in DMSO at 60 °C to provide **CP3**. The HPLC analysis of this peptide showed one single peak (Figure S1), confirming its purity, which did not require further purification. Our initial studies were directed to demonstrate the ability of this new D,L-α,β-CP hybrid to assemble into nanotubes both in solution and solid-state. **CP3** was soluble in double-distilled water, whose resulting pH (3–5) depended on CP concentration as a consequence of its protonation state after the HPLC purification. At neutral pH (Hepes buffer), the solubility is reduced, starting to precipitate at concentrations above 400 μM. The fluorescence spectra at native pH showed a band centered around 475 nm whose intensity slightly decreases as pH is raised until a critical point (pH 7.3), after which it increases again upon further base addition (Figure S2). Such behavior might be explained by the imidazolium ring deprotonation as the pH increases that might trigger the CP self-assembly. This piling up of CPs must cause the stacking of the aromatic fluorophore and, consequently, leading to higher fluorescent output. Experiments using Nile red (NR) were also carried out to determine the critical aggregation concentration (*cac*), the lowest concentration in which CP assembling starts to take place. NR is a hydrophobic dye that exhibits a significant increase together with a blue shift of the maximum emission wavelength when incorporated in hydrophobic environments.[30] The fluorescence experiments of **CP3** at different concentrations (6–500 μM) in Hepes (10 mM, pH 7) in the presence of NR (1 μM) allowed to estimate a *cac* around 50 μM (Figure 1a and S3). A similar value (45 μM) was obtained using the ThT probe in the same conditions (Figure S4),[31] suggesting that the β-sheet formation takes place together with hydrophobic packing when the aggregation occurs.

FTIR measurement was carried out to investigate the CP structure (Figure S5). The FTIR spectrum on a freeze-dried powder after basification supports the formation of a parallel β-sheet structure with a strong peak at 1633 cm^{-1} and a shoulder at 1664 cm^{-1}.[32] The amide A band at 3293 cm^{-1} is highly indicative of a well-established network of backbone-backbone hydrogen bonds.[33] CD studies were also performed to evaluate the pH-induced supramolecular self-assembly (Figure 1b). No CD signals were detected at native pH (ca. 3.6). On the contrary, a strong Cotton effect was observed at 255 nm and, to a lesser extent, for the Ant band at 340–400 nm as the pH increases. Such an outcome suggests the formation of long-range-ordered supramolecular assemblies as the pH increased, with the concomitant transfer of chirality from the peptide to the anthracene unit. Plotting the CD signal at 275 nm as a function of the pH (Figure S6) provided mean values of $pK_a = 7.3$ and a Hill coefficient of $n = 1.6 \pm 0.3$, suggesting a cooperative self-assembly process.

STEM microscopy was employed to evaluate the self-assembled structure of **CP3** at different pH (Figure 1c). As mentioned above, at native pH (3–5), the deposition of **CP3** solution (350 μM) on Cu grids provided mainly amorphous aggregates or, to a lesser extent, small tubes with diameters of about 2–3 nm and lengths ranging between 150–200 nm (Figure S7). This behavior was expected since the protonation

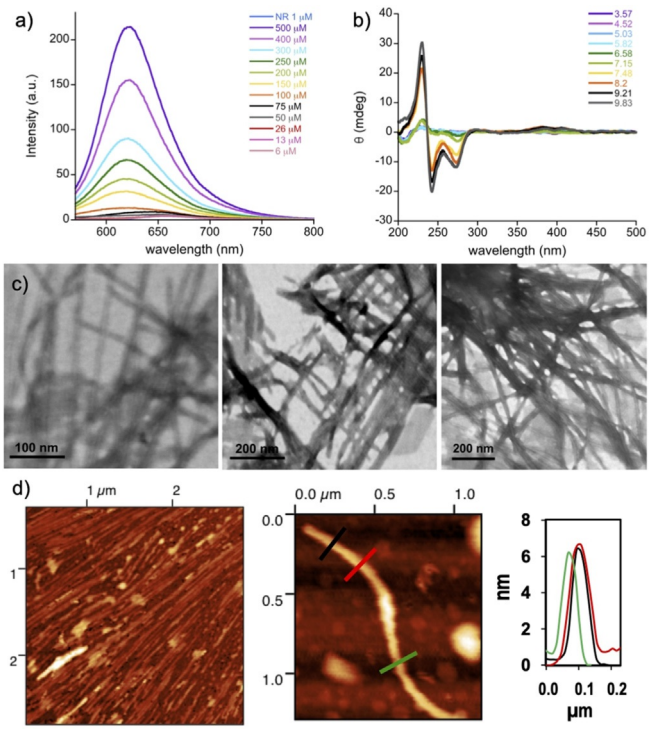

Figure 1. a) NR (1 μM) fluorescence spectra at different concentrations of **CP3** (10 mM Hepes, pH 7); b) Overlaid CD spectra of **CP3** aqueous solution at different pH; c) STEM micrographs achieved by deposition from solutions of **CP3** (350 μM, pH 7) on Cu grids. Staining was obtained with 2% w/v phosphotungstic acid (PTA). d) AFM micrographs of **CP3** (350 μM, pH 7) on a silicon wafer substrate. The height profiles (right) were achieved along the color lines shown in the image.

of the His side chains and the corresponding repulsive intermolecular interactions of charged imidazolium rings would preclude the build-up of nanotubes. On the other hand, at neutral pH (350 μM), individual SCPNs with a diameter of approximately 2–3 nm and lengths of a few microns together with bundles of them with an average diameter of ca. 5–6 nm were observed (Figure 1c). AFM analysis also corroborated these dimensions (Figure 1d and S8). Nanotube bundles must arise from intermolecular anthracene-anthracene interactions and the coexistence of both types of structure corroborate the existence of the mentioned hierarchical assembling process illustrated in Scheme 2. Therefore, the neutralization of aqueous media fosters the formation of a unique synergistic interplay between hydrogen bonding, hydrophobic, and π-π interactions with subsequent organization in hierarchical tubular architectures.

Once confirmed the nanotube formation, we started to evaluate the Ant photodimerization.[21] Therefore, we decided to investigate it upon UV irradiation at 350 nm at different pH (Figure S9): acidic (1.85), native (4.95), and neutral (Hepes, 10 mM). The degassed solutions of **CP3** (250 μM) were irradiated, and the process was followed by the reduction in absorption of the band at 386 nm due to the loss of aromaticity of anthracene moiety upon the [4+4] photochemical cycloaddition.[34] The reaction proceeds smoothly at pH 7 after 90 min. At native (4.95) and acidic

conditions (1.85), the conversion was smaller, 80 % and 60 %, respectively. The kinetic studies (Figure S10) allowed estimating a velocity constant k_1 of 0.14 min^{-1} at neutral pH, five times faster than for acidic conditions (0.03 min^{-1} at pH 1.85). These results suggest that Ant preorganization, favored at the conditions in which nanotubes are already forms, speeding up, as expected, the [4+4] cycloaddition. To confirm that these differences in rates are related with nanotube structure and not with media conditions, a model anthracene derivative (**Ant1**, Scheme 4) was prepared and UV irradiation at different pH (3.5 and 7.0) were carried out (Figures S11 and S12). The reactions of model **Ant1** at both pH are slower than for **CP3**. Additionally, and contrary to what was observed for **CP3**, the reaction is slower at neutral pH than at acidic media. This confirms the importance of the nanotube induced preorganization of Ant moieties to facilitate the photodimerization.

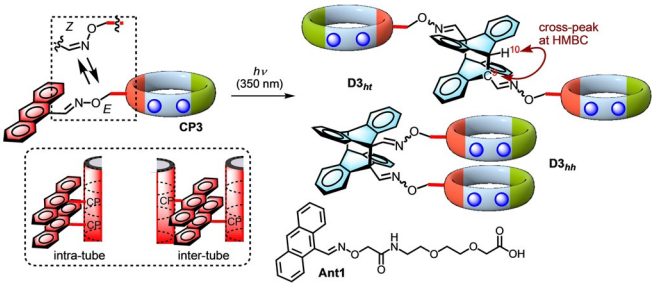

Scheme 4. Light-induced dimerization studies of **CP3** and proposed model for the formation of the initially proposed dimers, the head-to-head (**D3**$_{hh}$) derived from an intratubular process and the head to tail (**D3**$_{ht}$) generated by the inter-tubular interactions.

HPLC analysis of the mixture at pH 7, provided information regarding products formation (Figure S13). In addition to the starting material, four new peaks were observed during the irradiation process. One of them (min 8.59, Figure S13) raised very fast at the initial stage of irradiation to decrease later as the other three products start rising. Ms analysis (Figure S14) shows that this product has the molecular weight of the monomer, whose absorption spectra coincide with anthracene derivatives (Figure S15a). These suggest that this product must be a stereomer of starting material (**CP3**$_Z$). However, the molecular weight of the other three products (Figure S14) coincides with dimeric structures (**D3**) and whose UV spectra also confirm the [4+4] cycloadduct structures (Figure S15b). Additionally, to rule out the formation of photooxygenated products,[35] the reaction was also carried out in an oxygen-equilibrated solution at pH 7 (Figure S16). Under these conditions a variety of new products, some of them assigned to the corresponding endoperoxides and/or anthroquinones, were formed. Any of these products were not detected under the oxygen-free irradiation conditions.

The NMR analysis (Figure S17) of the newly formed monomer (**CP3**$_Z$) suggested that the thermodynamic oxyme *E*-isomer is photo-transformed into the *Z*-form[36] that is kinetically stable remaining in this geometry even when its aqueous solution is allowed to equilibrate on the bench for a few days. The observed shielding effect on the Lys side-chain protons, NH at 6.92 ppm or methylenes at 1.00 ($^{\gamma}CH_2$) and 1.17 ($^{\delta}CH_2$) ppm, derived from the ring current of Ant moiety (inset Scheme 3) suggest that the hydrophobic contacts must stabilize this form (Figure S17b).

In our initial evaluation, we considered the formation of two types of dimers,[37] the head-to-head (**D3**$_{hh}$) and the head-to-tail (**D3**$_{ht}$), based on whether the reaction occurs through inter-tubular or intra-tubular processes (Scheme 4). However, NMR analysis of the resulting dimers, obtained in a 1:2:4 ratio, rules out the formation or isolation of **D3**$_{hh}$ based on the observed cross-signal in the HMBC spectra between H_{10} and the bridgehead carbon C_9 (Scheme 4), see supporting information for further details. In order to discard the formation of the head-to-head dimer (**D3**$_{hh}$) that because of its instability could revert under the analysis conditions, a new experiment was carried out using combination of irradiation and dark cycles (Figure S18).[38] The formation of the head-to-head photodimer can be analyzed by following the changes of the anthracene absorption band (386 nm) upon sequential cycles of irradiation at 350 nm for a short time followed by an equilibration time in the dark at 298 K. Under these conditions no return of the anthracene absorption band was observed confirming that **D3**$_{hh}$ was not formed under these conditions. Consequently, all three isomers are head-to-tail derivatives differentiated by the geometry of oxyme bond: the *E*,*E*-, *Z*,*Z*- and *E*,*Z*-derivatives. The complexity of the spectrum of the major isomer (8.26 min) compared with the other two suggests that this corresponds to the ***E*,*Z*-D3**$_{ht}$ (Figure S17c). The ***Z*,*Z*-D3**$_{ht}$ was assigned to the minor product (5.37 min) according, again, to the shielding effect of the Lys side-chain protons (Figure S17e). Therefore, in the intertubular cycloaddition process, it seems that the more favorable packing is the one in which one *Z*-isomer is close to the *E*-derivative.

These dimers can be reverted to the Ant structure by heating the aqueous solutions containing each of the dimers (250 μM) for 800 min at 80 °C. The process was followed by UV-VIS (Figure S19) and HPLC (Figure S20) analysis. Interestingly, each of the dimers reverted into the corresponding monomers maintaining their hydrazone geometry without isomerization to the more stable form. The stability of the corresponding dimers (Figure S19) is quite different, while ***Z*,*Z*-D3**$_{ht}$ only provided a 12 % of the **CP3**$_Z$ after 800 min of heating, the heterodimeric form (***E*,*Z*-D3**$_{ht}$) provided almost a 50 % of free anthracene derivatives (**CP3**$_E$ and **CP3**$_Z$).

After confirming the dimerization process, we decided to study the self-assembly process at the macroscopic level. Therefore, solutions of **CP3** (350 μM) at neutral pH were analyzed by epifluorescence microscopy (Figure 2 and S21). Under these conditions, bright and green needle-shaped structures (∅ 1.5–2 μm) were observed denoting that the pH triggered hierarchical assembly process was maintained from the nanotubes to the micro-scale tubular architectures. Notably, by increasing the irradiation time, the fluorescence emission of the bundles switched irreversibly from green to blue (Figure 2 b and S22). Besides, the change in fluorescence

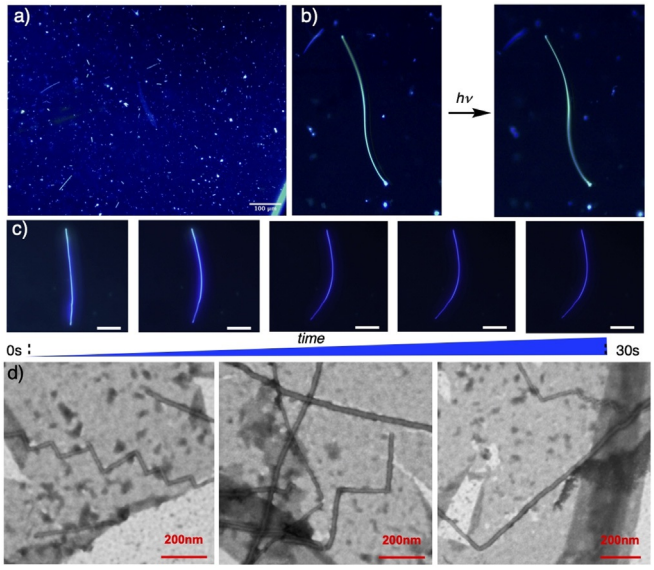

Figure 2. a) Epifluorescence images of **CP3** (350 μM, pH 8). b) Selected epifluorescence images of **CP3** nanotubes exposed to increasing irradiation time. Scale bar: 10 μm. c) Bending motion of the nanorods resulting from increased irradiation time. Scale bar: 25 μm. d) STEM micrographs of a solution of **CP3** (250 μM, pH 7) after irradiation for 90 min.

emission was associated in the larger fibres with a light-induced bending motion of the rods (Figure 2c). The differences in reaction time observed between the bulk solution (90 min) with the single fiber (30 s) must be related with the differences between the intra-bundle photochemical reaction and the combination of intra-bundle and inter-tubular dimerization that must take place in solution. At this respect, at the CP concentration used in the photodimerization reaction (250–350 μM) the single SCPNs are in equilibria with nanotubes bundles (Figure 2c) as can be inferred from the concentration dependent experiments carried out by UV/Vis and CD with a model peptide bearing a pyrene moiety (Figure S23).[39] The experiments carried out by UV/Vis in the presence of NR provide information about nanotube formation, while the appearance of the Cotton effect at 340–400 nm must be related with the nanotube bundling. The *cac* determined for each technique differ in almost one order of magnitude (10 μM and 100 μM), suggesting that they are measuring different aggregation events.

The resulting irradiated solutions were also evaluated by STEM (Figure 2d and S24). To our delight, zigzagging-shaped tubular structures were observed, suggesting that the light-induced process provided structures that retained the tubular structure but a variety of elbow in these hollow fibers were observed. Therefore, the light-induced anthracene dimerization is able to change the inter-nanotube packing, forcing to bend to satisfy the structural restrictions induced by the cycloadduct formation.

Conclusion

We have shown a new class of cyclic peptide hybrids designed to stack in a parallel fashion to form nanotubes that can bend as a result of a light stimulus. Under these conditions, the anthracene pendant that bears each cyclic component photodimerize, and the changes in dimensions that accompanies this cycloaddition perhaps together with *E*-*Z* oxyme isomerization induce structural changes in the nanotube packing that force the nanotube to curve. We envisage that these light-induced dynamic changes in shape can enable new functions, particularly in a biological context.

Acknowledgements

This work was supported by the Spanish Agencia Estatal de Investigación (AEI) (CTQ2016-78423-R and PID2019-111126RB-100), the Xunta de Galicia (ED431C 2017/25 and Centro singular de Investigación de Galicia accreditation 2019–2022, ED431G 2019/03), and the European Union (European Regional Development Fund—ERDF). We also thank the ORFEO-CINCA network and Mineco (CTQ2016-81797-REDC, and RED2018-102331-T).

Conflict of Interest

The authors declare no conflict of interest.

Keywords: cyclic peptides · molecular plumbing · nanotubes · photodimerization · self-assembly

[1] a) L. O. Björn, *Photobiology: the Science of Light and Life*, New York, Springer, **2015**; b) K. Glusac, *Nat. Chem.* **2016**, *8*, 734–735.
[2] a) W. K. Smith, T. C. Vogelmann, E. H. DeLucia, D. T. Bell, K. A. Shepherd, *BioScience* **1997**, *47*, 785–793; b) K. Palczewski, *Invest. Ophthalmol. Visual Sci.* **2014**, *55*, 6651–6672; c) E. S. Burgie, R. D. Vierstra, *Plant Cell* **2014**, *26*, 4568–4583.
[3] a) H. Kandori, K. Inoue, S. P. Tsunoda, *Chem. Rev.* **2018**, *118*, 10646–10658; b) O. P. Ernst, D. T. Lodowski, M. Elstner, P. Hegemann, L. S. Brown, H. Kandori, *Chem. Rev.* **2014**, *114*, 126–163; c) K. Murabe, T. Tsukamoto, T. Aizawa, M. Demura, T. Kikukawa, *J. Am. Chem. Soc.* **2020**, *142*, 16023–16030.
[4] a) F. Lancia, A. Ryabchun, N. Katsonis, *Nat. Rev. Chem.* **2019**, *3*, 536–551; b) A. Sorrenti, J. Leira-Iglesias, A. Sato, T. M. Hermans, *Nat. Commun.* **2017**, *8*, 15899; c) O. Shyshov, R.-C. Brachvogel, T. Bachmann, R. Srikantharajah, D. Segets, F. Hampel, R. Puchta, M. von Delius, *Angew. Chem. Int. Ed.* **2017**, *56*, 776–781; *Angew. Chem.* **2017**, *129*, 794–799; d) S. A. P. van Rossum, M. Tena-Solsona, J. H. van Esch, R. Eelkema, J. Boekhoven, *Chem. Soc. Rev.* **2017**, *46*, 5519–5535; e) B. A. Grzybowski, K. Fitzner, J. Paczesny, S. Granick, *Chem. Soc. Rev.* **2017**, *46*, 5647–5678; f) C. Pezzato, C. Cheng, J. F. Stoddart, R. D. Astumian, *Chem. Soc. Rev.* **2017**, *46*, 5491–5507; g) S. Kassem, T. van Leeuwen, A. S. Lubbe, M. R. Wilson, B. L. Feringa, D. A. Leigh, *Chem. Soc. Rev.* **2017**, *46*, 2592–2621; h) E. Mattia, S. Otto, *Nat. Nanotechnol.* **2015**, *10*, 111–119.
[5] a) M. W. Urban, *Handbook of Stimuli-Responsive Materials*, Wiley-VCH, Singapore, **2011**; b) Q. Li, A. P. H. J. Schenning, T. J. Bunning, *Adv. Opt. Mater.* **2019**, *7*, 1901160; c) J. J. van Thor, T. Gensch, K. J. Hellingwerf, L. N. Johnson, *Nat. Struct. Biol.*

2002, *9*, 37 – 41; d) N. A. Anderson, J. J. Shiang, R. J. Sension, *J. Phys. Chem. A* **1999**, *103*, 10730 – 10736; e) W. J. Schreier, T. E. Schrader, F. O. Koller, P. Gilch, C. E. Crespo-Hernández, V. N. Swaminathan, T. Carell, W. Zinth, B. Kohler, *Science* **2007**, *315*, 625 – 629.

[6] a) J. del Barrio, C. Sánchez-Somolinos, *Adv. Opt. Mater.* **2019**, *7*, 1900598; b) M. A. C. Stuart, W. T. S. Huck, J. Genzer, M. Müller, C. Ober, M. Stamm, G. B. Sukhorukov, I. Szleifer, V. V. Tsukruk, M. Urban, F. Winnik, S. Zauscher, I. Luzinov, S. Minko, *Nat. Mater.* **2010**, *9*, 101 – 113; c) K. Jung, N. Corrigan, M. Ciftci, J. Xu, S. E. Seo, C. J. Hawker, C. Boyer, *Adv. Mater.* **2020**, *32*, 1903850; d) G. Cheng, J. Perez-Mercader, *Chem* **2020**, *6*, 1160 – 1171.

[7] a) R. Göstl, A. Senf, S. Hecht, *Chem. Soc. Rev.* **2014**, *43*, 1982 – 1996; b) C. Dugave, L. Demange, *Chem. Rev.* **2003**, *103*, 2475 – 2532; c) V. Ramamurthy, B. Mondal, *J. Photochem. Photobiol. C* **2015**, *23*, 68 – 102.

[8] a) A. N. Volkov, T. Shiga, D. Nicholson, J. Shiomi, L. V. Zhigilei, *J. Appl. Phys.* **2012**, *111*, 053501; b) S. Tawfick, A. J. Hart, M. De Volder, *Nanoscale* **2012**, *4*, 3852 – 3856; c) B. Faria, N. Silvestre, J. N. C. Lopes, *Mech. Res. Commun.* **2016**, *73*, 19 – 24.

[9] T. Kim, L. Zhu, R. O. Al-Kaysi, C. J. Bardeen, *ChemPhysChem* **2014**, *15*, 400 – 414.

[10] a) N. Rodríguez-Vázquez, M. Amorín, J. R. Granja, *Org. Biomol. Chem.* **2017**, *15*, 4490 – 4505; b) I. W. Hamley, *Angew. Chem. Int. Ed.* **2014**, *53*, 6866 – 6881; *Angew. Chem.* **2014**, *126*, 6984 – 7000; c) Q. Song, Z. Cheng, M. Kariuki, S. C. L. Hall, S. K. Hill, J. Y. Rho, S. Perrier, *Chem. Rev.* **2021**, https://doi.org/10.1021/acs.chemrev.0c01291.

[11] M. R. Ghadiri, J. R. Granja, R. A. Milligan, D. E. McRee, N. Khazanovich, *Nature* **1993**, *366*, 324 – 327.

[12] a) M. R. Ghadiri, J. R. Granja, L. K. Buehler, *Nature* **1994**, *369*, 301 – 304; b) J. Montenegro, M. R. Ghadiri, J. R. Granja, *Acc. Chem. Res.* **2013**, *46*, 2955 – 2965; c) N. Rodríguez-Vázquez, H. L. Ozores, A. Guerra, E. González-Freire, A. Fuertes, M. Panciera, J. M. Priegue, J. Outeiral, J. Montenegro, R. García-Fandiño, M. Amorín, J. R. Granja, *Curr. Top. Med. Chem.* **2014**, *14*, 2647 – 2661; d) J. R. Granja, M. R. Ghadiri, *J. Am. Chem. Soc.* **1994**, *116*, 10785 – 10786; e) J. Sánchez-Quesada, H. S. Kim, M. R. Ghadiri, *Angew. Chem. Int. Ed.* **2001**, *40*, 2503 – 2506; *Angew. Chem.* **2001**, *113*, 2571 – 2574; f) M. Danial, C. M. N. Tran, K. A. Jolliffe, S. Perrier, *J. Am. Chem. Soc.* **2014**, *136*, 8018 – 8026; g) A. Fuertes, H. L. Ozores, M. Amorín, J. R. Granja, *Nanoscale* **2017**, *9*, 748 – 753.

[13] a) J. D. Hartgerink, J. R. Granja, R. A. Milligan, M. R. Ghadiri, *J. Am. Chem. Soc.* **1996**, *118*, 43 – 50; b) T. F. A. De Greef, M. M. J. Smulders, M. Wolffs, A. P. H. J. Schenning, R. P. Sijbesma, E. W. Meijer, *Chem. Rev.* **2009**, *109*, 5687 – 5754.

[14] a) J. Y. Rho, S. Perrier, *ACS Macro Lett.* **2021**, *10*, 258 – 271; b) S. Catrouillet, J. C. Brendel, S. Larnaudie, T. Barlow, K. A. Jolliffe, S. Perrier, *ACS Macro Lett.* **2016**, *5*, 1119 – 1123; c) R. Chapman, M. L. Koh, G. G. Warr, K. A. Jolliffe, S. Perrier, *Chem. Sci.* **2013**, *4*, 2581 – 2589; d) J. Y. Rho, J. C. Brendel, L. R. MacFarlane, E. D. H. Mansfield, R. Peltier, S. Rogers, M. Hartlieb, S. Perrier, *Adv. Funct. Mater.* **2017**, *27*, 201704569.

[15] R. J. Mart, R. K. Allemann, *Chem. Commun.* **2016**, *52*, 12262 – 12277.

[16] C. Li, A. Iscen, L. C. Palmer, G. C. Schatz, S. I. Stupp, *J. Am. Chem. Soc.* **2020**, *142*, 8447 – 8453.

[17] a) J. Yang, J.-I. Song, Q. Song, J. Y. Rho, E. D. H. Mansfield, S. C. L. Hall, M. Sambrook, F. Huang, S. Perrier, *Angew. Chem. Int. Ed.* **2020**, *59*, 8860 – 8863; *Angew. Chem.* **2020**, *132*, 8945 – 8948; b) A. Méndez-Ardoy, A. Bayón-Fernández, Z. Yu, C. Abell, J. R. Granja, J. Montenegro, *Angew. Chem. Int. Ed.* **2020**, *59*, 6902 – 6908; *Angew. Chem.* **2020**, *132*, 6969 – 6975; c) N. Cissé, T. Kudernac, *ChemSystemsChem* **2020**, *2*, 2000012; d) Q. Song, J. Yang, S. C. L. Hall, P. Gurnani, S. Perrier, *ACS Macro Lett.* **2019**, *8*, 1347 – 1352; e) S. M. Darnall, C. Li, M. Dunbar, M. Alsina, S. Keten, B. A. Helms, T. Xu, *J. Am. Chem. Soc.* **2019**, *141*, 10953 – 10957; f) M. Hartlieb, S. Catrouillet, A. Kuroki, C. Sanchez-Cano, R. Peltier, S. Perrier, *Chem. Sci.* **2019**, *10*, 5476 – 5483.

[18] A. Méndez-Ardoy, J. R. Granja, J. Montenegro, *Nanoscale Horiz.* **2018**, *3*, 391 – 396.

[19] M. Cuerva, R. García-Fandiño, C. Vázquez-Vázquez, M. A. López-Quintela, J. Montenegro, J. R. Granja, *ACS Nano* **2015**, *9*, 10834 – 10843.

[20] a) Q. Li, Z. Li, *Adv. Sci.* **2017**, *4*, 1600484; b) A. Das, A. Danao, S. Banerjee, A. M. Raj, G. Sharma, R. Prabhakar, V. Srinivasan, V. Ramamurthy, P. Sen, *J. Am. Chem. Soc.* **2021**, *143*, 2025 – 2036, and references therein; c) L. Fabbrizzi, A. Poggi, *Chem. Soc. Rev.* **1995**, *24*, 197 – 202.

[21] a) D. E. Applequist, R. L. Litle, E. C. Friedrich, R. E. Wall, *J. Am. Chem. Soc.* **1959**, *81*, 452 – 456; b) H. D. Becker, *Chem. Rev.* **1993**, *93*, 145 – 172; c) H. Bouas-Laurent, A. Castellan, J.-P. Desvergnea, R. Lapouyadec, *Chem. Soc. Rev.* **2000**, *29*, 43 – 55; d) H. Bouas-Laurent, A. Castellan, J.-P. Desvergnea, R. Lapouyadec, *Chem. Soc. Rev.* **2001**, *30*, 248 – 263; e) M. Yoshizawa, J. K. Klosterman, *Chem. Soc. Rev.* **2014**, *43*, 1885 – 1898.

[22] a) Z. Hou, W. M. Nau, R. Hoogenboom, *Polym. Chem.* **2021**, *12*, 307 – 315; b) Z. Jiang, M. L. Tan, M. Taheri, Q. Yan, T. Tsuzuki, M. G. Gardiner, B. Diggle, L. A. Connal, *Angew. Chem. Int. Ed.* **2020**, *59*, 7049 – 7056; *Angew. Chem.* **2020**, *132*, 7115 – 7122; c) A. Urushima, D. Taura, M. Tanaka, N. Horimoto, J. Tanabe, N. Ousaka, T. Mori, E. Yashima, *Angew. Chem. Int. Ed.* **2020**, *59*, 7478 – 7486; *Angew. Chem.* **2020**, *132*, 7548 – 7556; d) P. R. A. Chivers, R. S. Dookie, J. Gough, S. Webb, *Chem. Commun.* **2020**, *56*, 13792 – 13795; e) W. Zhou, Y. Chen, Q. Yu, P. Li, X. Chen, *Chem. Sci.* **2019**, *10*, 3346 – 3352; f) J. Bai, Z. Shi, J. Yin, M. Tian, R. Qu, *Adv. Funct. Mater.* **2018**, *28*, 1800939; g) Z. Gao, Y. Han, F. Wang, *Nat. Commun.* **2018**, *9*, 3977; h) A. Saruwatari, R. Tamate, H. Kokubo, M. Watanabe, *Chem. Commun.* **2018**, *54*, 13371 – 13374; i) Z.-A. Huang, C. Chen, X.-D. Yang, X.-B. Fan, W. Zhou, C.-H. Tung, L.-Z. Wu, H. Cong, *J. Am. Chem. Soc.* **2016**, *138*, 11144 – 11147; j) N. Kishi, M. Akita, M. Kamiya, S. Hayashi, H.-F. Hsu, *J. Am. Chem. Soc.* **2013**, *135*, 12976 – 12979.

[23] a) T. Salzillo, A. Brillante, *CrystEngComm* **2019**, *21*, 3127 – 3136; b) M. Li, A. D. Schlüter, J. Sakamoto, *J. Am. Chem. Soc.* **2012**, *134*, 11721 – 11725.

[24] Y. I. A. H. Fujita, *J. Org. Chem.* **1997**, *61*, 5677 – 5680.

[25] a) M. R. Silk, J. Newman, J. C. Ratcliffe, J. F. White, T. Caradoc-Davies, J. R. Price, S. Perrier, P. E. Thompson, D. K. Chalmers, *Chem. Commun.* **2017**, *53*, 6613 – 6616; b) M. Calvelo, A. Lamas, A. Guerra, M. Amorín, R. García-Fandiño, J. R. Granja, *Chem. Eur. J.* **2020**, *26*, 5846 – 5858.

[26] a) M. Panciera, E. González-Freire, M. Calvelo, M. Amorín, J. R. Granja, *Pept. Sci.* **2020**, *112*, e24132; b) N. Rodríguez-Vázquez, R. García Fandiño, M. J. Aldegunde, J. Brea, M. I. Loza, M. Amorín, J. R. Granja, *Org. Lett.* **2017**, *19*, 2560 – 2563; c) M. Panciera, M. Amorín, L. Castedo, J. R. Granja, *Chem. Eur. J.* **2013**, *19*, 4826 – 4834; d) Y. Ishihara, S. Kimura, *Biopolymers* **2012**, *98*, 155 – 160; e) R. Hourani, C. Zhang, R. van der Weegen, L. Ruiz, C. Li, S. Keten, B. A. Helms, T. Xu, *J. Am. Chem. Soc.* **2011**, *133*, 15296 – 15297; f) C. Reiriz, R. J. Brea, R. Arranz, J. L. Carrascosa, A. Garibotti, B. Manning, J. M. Valpuesta, R. Eritja, L. Castedo, J. R. Granja, *J. Am. Chem. Soc.* **2009**, *131*, 11335 – 11337.

[27] R. P. Cheng, S. H. Gellman, W. F. DeGrado, *Chem. Rev.* **2001**, *101*, 3219 – 3232.

[28] a) D. Seebach, J. L. Matthew, T. W. A. Meden, C. Baerlocher, L. B. McCusker, *Helv. Chim. Acta* **1997**, *80*, 173 – 182; b) T. D. Clark, L. K. Buehler, M. R. Ghadiri, *J. Am. Chem. Soc.* **1998**, *120*, 651 – 656; c) T. Marmin, Y. L. Dory, *Chem. Eur. J.* **2019**, *25*, 6707 – 6711; d) S. Leclair, P. Baillargeon, R. Skouta, D. Gauthier, Y. Zhao, Y. L. Dory, *Angew. Chem. Int. Ed.* **2004**, *43*, 349 – 353;

Angew. Chem. **2004**, *116*, 353 – 357; e) Y. Tabata, Y. Kamano, H. Uji, T. Imai, S. Kimura, *Chem. Lett.* **2019**, *48*, 322 – 324.
[29] J. M. Priegue, J. Montenegro, J. R. Granja, *Small* **2014**, *10*, 3613 – 3618.
[30] a) R. M. P. Da Silva, D. Van Der Zwaag, L. Albertazzi, S. S. Lee, E. W. Meijer, S. I. Stupp, *Nat. Commun.* **2016**, *7*, 11561; b) R. Mishra, D. Sjölander, P. Hammarström, *Mol. BioSyst.* **2011**, *7*, 1232 – 1240; c) M. C. A. Stuart, J. C. van de Pas, J. B. F. N. Engberts, *J. Phys. Org. Chem.* **2005**, *18*, 929 – 934.
[31] a) H. Naiki, K. Higuchi, M. Hosokawa, T. Takeda, *Anal. Biochem.* **1989**, *177*, 244 – 249; b) M. Girych, G. Gorbenko, I. Maliyov, V. Trusova, C. Mizuguchi, H. Saito, P. Kinnunen, *Methods Appl. Fluoresc.* **2016**, *4*, 034010.
[32] a) H. S. Kim, J. D. Hartgerink, M. R. Ghadiri, *J. Am. Chem. Soc.* **1998**, *120*, 4417 – 4424; b) J. Kubelka, T. A. Keiderling, *J. Am. Chem. Soc.* **2001**, *123*, 12048 – 12058; c) Y. Zou, Y. Li, W. Hao, X. Hu, G. Ma, *J. Phys. Chem. B* **2013**, *117*, 4003 – 4013.
[33] S. Krimm, J. Bandekar in *Advances in Protein Chemistry*, *Vol. 38* (Eds.: C. B. Anfinsen, J. T. Edsall, F. M. Richards), Elsevier, Amsterdam, **1986**, pp. 181 – 364.
[34] C.-H. Tung, J.-Q. Guan, *J. Org. Chem.* **1998**, *63*, 5857 – 5862.
[35] a) W. Fudickar, T. Linker, *Chem. Eur. J.* **2011**, *17*, 13661 – 13664; b) W. Fudickar, T. Linker, *J. Am. Chem. Soc.* **2012**, *134*, 15071 – 15082; c) Y. Han, M. Liu, R. Zhong, Z. Gao, Z. Chen, M. Zhang, F. Wang, *Inorg. Chem.* **2019**, *58*, 12407 – 12414.
[36] a) H. D. Roth, *Light-Induced Chemistry of Oximes and Derivatives*, John Wiley & Sons, Ltd, Chichester, UK, **2010**; b) S. Mondal, P. Chakraborty, P. Bairi, D. P. Chatterjee, A. K. Nandi, *Chem. Commun.* **2015**, *51*, 10680 – 10683; c) B. Bai, M. Zhang, N. Ji, J. Wei, H. Wang, M. Li, *Chem. Commun.* **2017**, *53*, 2693 – 2696.
[37] a) A. Castellan, R. Lapouyade, H. Boutas-Laurent, J. Y. Laliemand, *Tetrahedron Lett.* **1975**, *29*, 2470 – 2475; b) X. Hu, F. Liu, X. Zhang, Z. Zhao, S. Liu, *Chem. Sci.* **2020**, *11*, 4779 – 4785; c) H. Matsumoto, Y. Nishimura, T. Arai, *Photochem. Photobiol. Sci.* **2012**, *15*, 1071 – 1079.
[38] A. Tron, P. J. Thornton, C. Lincheneau, J.-P. Desvergne, N. Spencer, J. H. R. Tucker, N. D. McClenaghan, *J. Org. Chem.* **2015**, *80*, 988 – 996.
[39] Although **CP3** provide similar behavior than the CP bearing the pyrene moiety (**CP3P**) its precipitation at concentration higher of 400 μM did not allowed to precisely estimate the critical aggregation concentration of bundle formation in the CD experiments.

Manuscript received: May 26, 2021
Accepted manuscript online: June 29, 2021
Version of record online: July 16, 2021

